2012

A Doubling Technique for the Power Method Transformations

Mohan D. Pant
University of Texas at Arlington

Todd C. Headrick
Southern Illinois University Carbondale, headrick@siu.edu

Recommended Citation

A Doubling Technique
for the Power Method Transformations

Mohan D. Pant

Department of Curriculum and Instruction, 320-B Science Hall
University of Texas at Arlington, Arlington, TX-76019, USA
mpant@uta.edu

Todd C. Headrick

Section on Statistics and Measurement, Department EPSE
222-J Wham Bldg., Southern Illinois University Carbondale
Carbondale, IL 62901-4618, USA
headrick@siu.edu

Abstract

Power method polynomials are used for simulating non-normal distributions with specified product moments or L-moments. The power method is capable of producing distributions with extreme values of skew (L-skew) and kurtosis (L-kurtosis). However, these distributions can be extremely peaked and thus not representative of real-world data. To obviate this problem, two families of distributions are introduced based on a doubling technique with symmetric standard normal and logistic power method distributions. The primary focus of the methodology is in the context of L-moment theory. As such, L-moment based systems of equations are derived for simulating univariate and multivariate non-normal distributions with specified values of L-skew, L-kurtosis, and L-correlation. Evaluation of the proposed doubling technique indicates that estimates of L-skew, L-kurtosis, and L-correlation are superior to conventional product-moments in terms of relative bias and relative efficiency when extreme non-normal distributions are of concern.

1   Introduction

The power method (PM) transformation [4, 6, 7] has been used in a variety of settings for the purpose of simulating non-normal distributions with specified product moments. Some examples include: asset pricing theory [1], toxicology research [17], price risk [25], business-cycle features [15], regression analysis [10], ANOVA [3, 23, 24], ANCOVA [5, 12], microarray analysis [30], multivariate analysis [32], item response theory [33], nonparametric statistics [2], and structural equation modeling [14]. The third-order PM transformation is defined as in [4, 6, 7].

$$p(Z) = c_0 + c_1 Z + c_2 Z^2 + c_3 Z^3 \tag{1}$$

where $Z \sim iidN(0,1)$ with standard normal probability density function (pdf) and cumulative distribution function (cdf) denoted as $\phi(z)$ and $\Phi(z)$. In order for (1) to produce a valid pdf it requires that the PM transformation be a strictly increasing monotone function [7, p. 12]. This requirement implies that an inverse function (p^{-1}) exists. As such, the cdf associated with (1) can be expressed as $F(p(z)) = \Phi(z)$ and subsequently differentiating this cdf with respect to z will yield the PM pdf as $f(p(z)) = \phi(z)/(p'(z))$. We would note that the PM cdf and pdf could also be expressed as $F(y) = \Phi(z)$ and $f(y) = \phi(z)/(p'(z))$, where $z = p^{-1}(y)$.

One of the limitations associated with the PM is that distributions with large values of skew and (or) kurtosis can be excessively leptokurtic and thus may not be representative of real world data. For example, Figure 1 (Panel A) gives a PM pdf with skew and kurtosis of $\gamma_3 = 4$ and $\gamma_4 = 40$. This example illustrates the limitation that the PM can have in terms of excessive peakedness.

Another limitation associated with the PM is that conventional estimators of γ_3 and γ_4 have unfavorable attributes insofar as they can be substantially biased, have high variance, or can be influenced by outliers [8, 16]. To address the latter limitation, the PM has been characterized in the context of L-moments [8]. Specifically, some of the advantages that L-moment based estimators (e.g., L-skew and L-kurtosis) have over conventional moments in the context of PM are that they (a) exist whenever the mean of the distribution exists, (b) are nearly unbiased for all sample sizes and distributions, and (c) are more robust in the presence of outliers [18-21].

Although the PM has been traditionally used for simulating non-normal distributions with controlled Pearson correlations (e.g. [6, 11, 36]; [7, p.29]), it also has limitations in this context. Specifically, the PM procedure is based on conventional product moments and the popular NORTA ([28]) approach,

which begins with generating multivariate standard normal deviates. The primary limitation associated with NORTA is that the Pearson correlation is not invariant under nonlinear strictly increasing transformations such as (1). As such, the NORTA approach must begin with the computation of an intermediate correlation (IC) matrix, which is different than the specified correlation matrix between the non-normal PM distributions. The purpose of the IC matrix is to adjust for the non-normalization effect of the transformation in (1) such that the resulting non-normal distributions have their specified skew, kurtosis, and specified correlation matrix. This requires the absolute values of the solved intermediate correlations to be greater than (or equal to) their associated specified Pearson correlations [36].
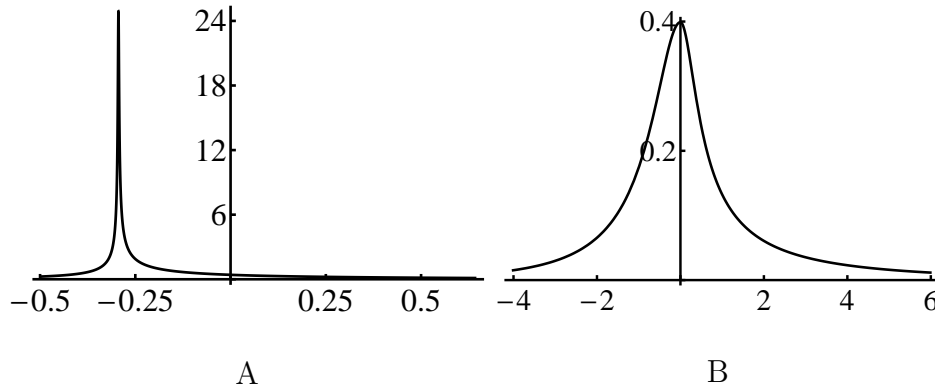
$$c_0 = -0.271450, c_1 = 0.130891,$$

$$c_2 = 0.271450, c_3 = 0.211277$$

$$C_{\mathcal{L}} = 0.307610, C_{\mathcal{R}} = 0.985795$$

Figure 1: Graphs of a traditional third order (Panel A) and a double-SN (Panel B) PM distributions based on matching the conventional skew of 4 and kurtosis of 40. The values of coefficients $c_{i=0,1,2,3}$ for the distribution in Panel A and the values of $C_{\mathcal{L}}$ and $C_{\mathcal{R}}$ for the distribution in Panel B were determined by solving systems of equations (2.20) and (2.21) from [7, p. 15] and equations (58) and (59) from the Appendix B, respectively.

Two other limitations associated with NORTA approach in this context are that solutions to an IC matrix may neither (a) exist in the range of [-1, +1], nor (b) yield a positive definite intermediate correlation matrix. To demonstrate, Table 1 gives a computed IC matrix based on four non-normal PM distributions and a specified positive definite correlation matrix. Inspection of this table demonstrates the problem associated with this IC matrix as it is not positive definite.

In view of the above, we introduce two families of L-moment based distributions that will ameliorate the problems of (a) excessive leptokurtic behavior that is associated with some PM distributions and (b) biased estimates of conventional measures of skew and kurtosis. These families of distributions are referred herein as the double-SN and the double-SL PMs and are based on a doubling technique as in [27]. Specifically, the double-SN PM family of distributions is a combination of two piecewise polynomials of standard normal-based transformations expressed as

$$p(Z) = \begin{cases} Z + C_{\mathcal{L}}Z^3, & \text{for } Z \leq 0 \\ Z + C_{\mathcal{R}}Z^3, & \text{for } Z \geq 0 \end{cases} \tag{2}$$

where $C_{\mathcal{L}} \geq 0$ and $C_{\mathcal{R}} \geq 0$. To demonstrate, Figure 1 (Panel B) shows the graph of a double-SN distribution which has the height of the standard normal distribution and $\gamma_3 = 4$, $\gamma_4 = 40$ and with corresponding parameters of L-skew and L-kurtosis of $\tau_3 = 0.2559$ and $\tau_4 = 0.4007$, respectively. Inspection of Figure 1 (Panels A and B) clearly indicates that these two PM distributions are markedly different even though both distributions have the same values of skew and kurtosis ($\gamma_3 = 4$, $\gamma_4 = 40$).

Further, another goal of this article is to extend the advantages of the L-moment-based PM [8] from univariate to multivariate non-normal data generation. Specifically, the purpose is to develop a methodology and a procedure for simulating non-normal double PM distributions with specified L-moments and controlled L-correlations. Two primary advantages of the proposed procedure are that intermediate correlations are less than, and in closer proximity to, their respective specified correlations and thus less likely than the traditional PM procedure to produce an IC matrix that is not positive definite. To demonstrate, inspection of Table 2 indicates that the problems associated with the intermediate correlation matrix in Table 1 are circumvented by the new L-moment-based procedure. More specifically, the solved values of intermediate correlations are in closer proximity to their respective specified correlations and comprise a positive definite matrix.

The remainder of the paper is outlined as follows. In Section 2, a summary of univariate L-moment theory is provided along with the derivations of the systems of equations for the double PM families. Also included in Section 2 is the derivation of a double-SL PM family based on standard logistic distribution, i.e., $W + C_{\mathcal{L}}W^3$ for $W \leq 0$ and $W + C_{\mathcal{R}}W^3$ for $W \geq 0$ in equation (2). In Section 3, an introduction to the coefficient of L-correlation is provided and the methodology for solving for intermediate correlations for specified L-correlations between the double PM distributions is presented. In Section 4, the steps for implementing the proposed L-moment procedure are described

for simulating non-normal double PM distributions with controlled skew (*L*-skew), kurtosis (*L*-kurtosis), and Pearson correlations (*L*-correlations). Numerical examples and the results of simulation are also provided to confirm the derivations and compare the new procedure with the traditional or conventional moment-based procedure. In Section 5, the results of the simulation are discussed.

	1	2	3	4
1	1			
2	0.688701 (0.60)	1		
3	0.781855 (0.70)	0.554625 (0.50)	1	
4	0.946869 (0.85)	0.753626 (0.70)	0.530600 (0.50)	1

Table 1: An *invalid* conventional moment-based intermediate correlation matrix for the distributions in Figure 3. The specified values of Pearson correlation are shown in the parentheses. The matrix of the solved intermediate correlations is not positive definite even though the matrix of specified correlations is positive definite

	1	2	3	4
1	1			
2	0.552568 (0.60)	1		
3	0.653742 (0.70)	0.464701 (0.50)	1	
4	0.816350 (0.85)	0.664034 (0.70)	0.474651 (0.50)	1

Table 2: A *valid* (positive definite) *L*-moment-based double PM intermediate correlation matrix for the distributions in Figure 3. The specified values of *L*-correlation in parentheses correspond to the same specified values of Pearson correlation in Table 1.

2 Methodology

2.1 Preliminaries

Let X be a continuous random variable from a distribution with cdf $F(x)$, pdf $f(x)$, and probability weighted moments (PWMs) expressed as

$$\beta_r = \int x\{F(x)\}^r f(x)dx. \tag{3}$$

The first four *L*-moments $(\lambda_{i=1,\dots,4})$ associated with X can be expressed as linear combinations of the PWMs as in Headrick [8] (see, also [18-21])

$$\lambda_1 \;=\; \beta_0 \tag{4}$$

$$\lambda_2 = 2\beta_1 - \beta_0 \tag{5}$$

$$\lambda_3 = 6\beta_2 - 6\beta_1 + \beta_0 \tag{6}$$

$$\lambda_4 = 20\beta_3 - 30\beta_2 + 12\beta_1 - \beta_0. \tag{7}$$

The coefficients associated with $\beta_{r=0,\dots,3}$ in (4)-(7) are determined from shifted orthogonal Legendre polynomials and are computed as shown in [21, p. 20] or in [8].

As with conventional moments, the L-moments λ_1 and λ_2 in (4) and (5) are measures of location and scale, which are the arithmetic mean and one-half the coefficient of mean difference. The third- and fourth-order L-moments are transformed to dimensionless L-moment ratios defined as $\tau_3 = \lambda_3/\lambda_2$ and $\tau_4 = \lambda_4/\lambda_2$ and are referred to as the indices of L-skew and L-kurtosis. In general, L-moment ratios are bounded in the interval of $-1 < \tau_r < 1$, for $r \geq 3$, where a symmetric distribution ($\tau_3 = 0$) implies that all L-moment ratios with odd subscripts are zero. Other smaller boundaries can be found for more specific cases. For example, for continuous distributions the index of L-kurtosis (τ_4) has the boundary condition of ([22])

$$\frac{5\tau_3{}^2 - 1}{4} < \tau_4 < 1. \tag{8}$$

2.2 L-moments for the double-standard normal (SN) PM distributions

The derivation of the L-moment-based system of equations begins with defining the PWMs based on (3) in terms of $p(Z)$ in (2) and the standard normal pdf $\phi(z)$ and cdf $\Phi(z)$ as

$$\beta_r = \int_{-\infty}^{0} (z + C_\mathcal{L}z^3)\{\Phi(z)\}^r \phi(z)dz + \int_{0}^{\infty} (z + C_\mathcal{R}z^3)\{\Phi(z)\}^r \phi(z)dz. \tag{9}$$

Integrating (9) for $r = 0$ and 1 and substituting into (4) and (5) gives

$$\lambda_1 = (C_\mathcal{R} - C_\mathcal{L})\sqrt{2/\pi} \tag{10}$$

$$\lambda_2 = \frac{4 + 5C_\mathcal{L} + 5C_\mathcal{R}}{4\sqrt{\pi}}. \tag{11}$$

In terms of deriving β_2, (9) can be further split into four parts as

$$\begin{aligned}
\beta_2 &= \int_{-\infty}^{0} z\{\Phi(z)\}^2 \phi(z)dz + C_\mathcal{L} \int_{-\infty}^{0} z^3\{\Phi(z)\}^2 \phi(z)dz \\
&\quad + \int_{0}^{\infty} z\{\Phi(z)\}^2 \phi(z)dz + C_\mathcal{R} \int_{0}^{\infty} z^3\{\Phi(z)\}^2 \phi(z)dz \\
&= I_1 + C_\mathcal{L}I_2 + I_3 + C_\mathcal{R}I_4. \tag{12}
\end{aligned}$$

where I_1, I_2, I_3, and I_4 in (12) are evaluated after several manipulations and are presented in the Appendix A. The values of these integrals are subsequently substituted into (12) to yield

$$\beta_2 = \frac{6\pi + 15\pi C_\mathcal{R} + (C_\mathcal{R} - C_\mathcal{L})\{\sqrt{2} + 3\sqrt{2}\pi - 15\tan^{-1}(\sqrt{2})\}}{12\pi^{3/2}}. \tag{13}$$

In terms of deriving β_3, it is convenient to consider the left and the right tails of the double-SN PM distribution separately. Thus,

$$\beta_3 = \beta_{3\mathcal{L}} + \beta_{3\mathcal{R}} \tag{14}$$

where $\beta_{3\mathcal{L}}$ and $\beta_{3\mathcal{R}}$ are obtained by separately solving the following two equations

$$\tau_{4\mathcal{L}} = \frac{\lambda_{4\mathcal{L}}}{\lambda_{2\mathcal{L}}} = \frac{20\beta_{3\mathcal{L}} - 30\beta_{2\mathcal{L}} + 12\beta_{1\mathcal{L}} - \beta_{0\mathcal{L}}}{\lambda_{2\mathcal{L}}} \tag{15}$$

$$\tau_{4\mathcal{R}} = \frac{\lambda_{4\mathcal{R}}}{\lambda_{2\mathcal{R}}} = \frac{20\beta_{3\mathcal{R}} - 30\beta_{2\mathcal{R}} + 12\beta_{1\mathcal{R}} - \beta_{0\mathcal{R}}}{\lambda_{2\mathcal{R}}} \tag{16}$$

where $\beta_{2\mathcal{L}} = I_1 + C_\mathcal{L}I_2$ and $\beta_{2\mathcal{R}} = I_3 + C_\mathcal{R}I_4$. The terms $\beta_{0\mathcal{L}}$, $\beta_{1\mathcal{L}}$ and $\beta_{0\mathcal{R}}$, $\beta_{1\mathcal{R}}$ are obtained by integrating (9) for $r = 0, 1$; the terms $\lambda_{2\mathcal{L}}$ and $\lambda_{2\mathcal{R}}$ are obtained using (5); and $\tau_{4\mathcal{L}}$ and $\tau_{4\mathcal{R}}$ are obtained from using Headrick's equation (2.17) [8, p. 7]. Thus, we have

$$\beta_{3\mathcal{L}} = \frac{12\tan^{-1}(\sqrt{2})(2 + 5C_\mathcal{L}) - (6 + \sqrt{2})\pi - C_\mathcal{L}\{\sqrt{2} + (15 + 2\sqrt{2})\pi\}}{16\pi^{3/2}} \tag{17}$$

$$\beta_{3\mathcal{R}} = \frac{(6 + \sqrt{2})\pi + C_\mathcal{R}\{3\sqrt{2} + (15 + 2\sqrt{2})\pi\}}{16\pi^{3/2}}. \tag{18}$$

Using (17) and (18) into (14), we obtain

$$\beta_3 = \frac{12\tan^{-1}(\sqrt{2})(2 + 5C_\mathcal{L}) + \sqrt{2}(3C_\mathcal{R} - C_\mathcal{L}) + (15 + 2\sqrt{2})(C_\mathcal{R} - C_\mathcal{L})\pi}{16\pi^{3/2}}. \tag{19}$$

Hence, substituting β_0, β_1, β_2, β_3 into (6) and (7) gives the terms for λ_3 and λ_4, which subsequently yield L-skew and L-kurtosis as follows

$$\tau_3 = \frac{(C_\mathcal{L} - C_\mathcal{R})\{-2\sqrt{2} + (2\sqrt{2} - 15)\pi + 30\tan^{-1}(\sqrt{2})\}}{(4 + 5C_\mathcal{L} + 5C_\mathcal{R})\pi} \tag{20}$$

$$\tau_4 = \frac{120\tan^{-1}(\sqrt{2}) - 36\pi + 5(C_{\mathcal{L}} + C_{\mathcal{R}})\{\sqrt{2} - 9\pi + 30\tan^{-1}(\sqrt{2})\}}{(4 + 5C_{\mathcal{L}} + 5C_{\mathcal{R}})\pi}. \quad (21)$$

As such, given specified values of τ_3 and τ_4, (20) and (21) can be numerically solved for the corresponding values of $C_{\mathcal{L}}$ and $C_{\mathcal{R}}$. Simple inspection of (20) and (21) indicates that interchanging values of $C_{\mathcal{L}}$ and $C_{\mathcal{R}}$ reverses the sign of τ_3 and has no effect on τ_4. Presented in Figure 2 (Panel A) is a graph of the region for possible combinations of $|\tau_3|$ and τ_4 in (20) and (21). Note that the graph in Figure 2 (Panel A) was drawn by setting $C_{\mathcal{L}} = 0$ with $C_{\mathcal{R}} \in [0, \infty)$ in (20) and (21). Specifically, Figure 2 (Panel A) shows the minimum value of τ_4 for the double-SN PM distributions as $min(\tau_4) \approx .1226$, where $C_{\mathcal{L}} = C_{\mathcal{R}} = C = 0$ and $\tau_3 = 0$, which are associated with the standard normal pdf. The maximum value of τ_4 is $max(\tau_4) \approx .5728$, which is the limiting value of τ_4 in (21) when $C_{\mathcal{L}} = C_{\mathcal{R}} \to \infty$, and is associated with the pdf of $p(Z) = (2/5)Z^3$ [9, p. 3]. Figure 3 provides an example of four double-SN PM distributions to demonstrate the methodology.
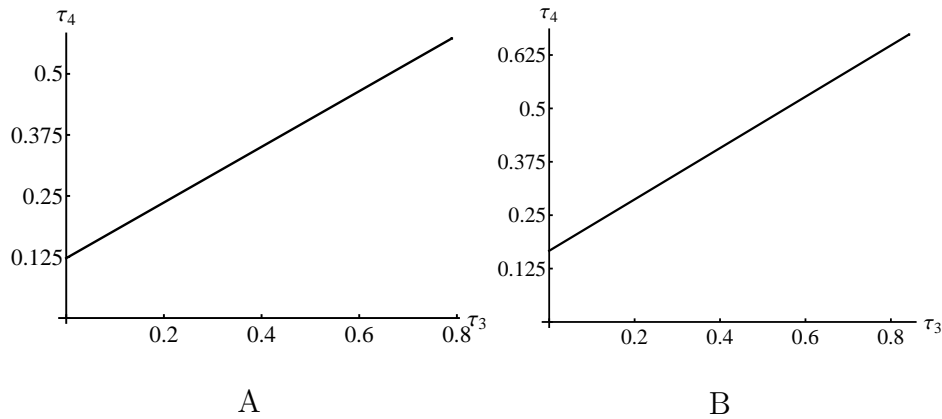
Figure 2: Boundary graphs of the regions for possible combinations of (absolute value) L-skew ($|\tau_3|$) and L-kurtosis (τ_4) for the double-SN (Panel A) and the double-SL (Panel B) PM distributions.

The conventional moment based system for the double-SN PM distributions is given in Appendix B. This system was used to solve for the values of $C_{\mathcal{L}}$ and $C_{\mathcal{R}}$ for specified values of γ_3 and γ_4 associated with the distributions in Figure 3. The solved values of $C_{\mathcal{L}}$ and $C_{\mathcal{R}}$ were eventually substituted into (20) and (21) to determine the values of τ_3 and τ_4. The four distributions in Figure 3 are used in simulation portion of the study in Section 4.

The unique solutions for $C_{\mathcal{L}}$ and $C_{\mathcal{R}}$ in (20) and (21) can also be obtained by evaluating the following expressions for specified values of τ_3 and τ_4 as

$$
\begin{aligned}
C_{\mathcal{L}} \;=\; & [(30 - 4\sqrt{2})\pi^2(9 + \tau_4) - 120(\sqrt{2} - 15d)d + 2\pi\{2(9\sqrt{2} + \tau_4(\sqrt{2} - 15d) \\
& + 30(\sqrt{2} - 12)d)\}]/[5(2\sqrt{2} - 15)\pi^2(9 + \tau_4) + 10\{2 + 15(\sqrt{2} - 30d)d\} \\
& - 5\pi\{4 + 3\sqrt{2} + 2\tau_4(\sqrt{2} - 15d) + 60(\sqrt{2} - 12)d\}]
\end{aligned}
\tag{22}
$$

$$
\begin{aligned}
C_{\mathcal{R}} \;=\; & [2\{-10\pi\tau_3 - ((30d - 2\sqrt{2} + \pi(2\sqrt{2} - 15 - 5\tau_3))\{60(\sqrt{2} - 15d)d \\
& + (2\sqrt{2} - 15)\pi^2(9 + \tau_4) + \pi(5\sqrt{2}\tau_3 - 2(9\sqrt{2} + \tau_4(\sqrt{2} - 15d) \\
& + 30(\sqrt{2} - 12)d)\}\}\}/\{4 + (2\sqrt{2} - 15)\pi^2(9 + \tau_4) + 30(\sqrt{2} - 15d)d \\
& - \pi(4 + 3\sqrt{2} + 2\tau_4(\sqrt{2} - 15d) + 60(\sqrt{2} - 12)d))\}] \\
& /[5\{30d - 2\sqrt{2} + \pi(2\sqrt{2} - 15 + 5\tau_3)\}]
\end{aligned}
\tag{23}
$$

where $d = \tan^{-1}(\sqrt{2})$ in (22) and (23).

2.3 L-moments for the double-standard logistic (SL) PM distributions

The derivation of L-moment-based system of equations for the double-SL PM distributions associated with (2) can be analogously determined based on the methodology presented in the previous section by evaluating the following integral

$$
\beta_r = \int_{-\infty}^{0} (w + C_{\mathcal{L}}w^3)\{\Phi(w)\}^r \phi(w)dw + \int_{0}^{\infty} (w + C_{\mathcal{R}}w^3)\{\Phi(w)\}^r \phi(w)dw. \tag{24}
$$

where $\phi(w) = (\pi/\sqrt{3})\exp\{-(\pi/\sqrt{3})w\}/(1 + \exp\{-(\pi/\sqrt{3})w\})^2$ and $\Phi(w) = (1 + \exp\{-(\pi/\sqrt{3})w\})^{-1}$ are the pdf and cdf associated with the standard logistic distribution.

Thus, integrating (24) for $r = 0, \ldots, 3$ and subsequently substituting the expressions for $\beta_0, \beta_1, \beta_2, \beta_3$ into (4)-(7) and simplifying yields the following system

$$
\lambda_1 = \frac{27\sqrt{3}(C_{\mathcal{R}} - C_{\mathcal{L}})\mathrm{Zeta}[3]}{2\pi^3} \tag{25}
$$

$$
\lambda_2 = \frac{\sqrt{3}(2 + 3C_{\mathcal{L}} + 3C_{\mathcal{R}})}{2\pi} \tag{26}
$$

$$
\tau_3 = \frac{18(C_{\mathcal{R}} - C_{\mathcal{L}})\ln 4}{(2 + 3C_{\mathcal{L}} + 3C_{\mathcal{R}})\pi^2} \tag{27}
$$

$$\tau_4 = \frac{1}{6} + \frac{15(C_{\mathcal{L}} + C_{\mathcal{R}})}{(2 + 3C_{\mathcal{L}} + 3C_{\mathcal{R}})\pi^2} \tag{28}$$

where Zeta[3] $= 1.202056903159594$ in (25).

For given values of τ_3 and τ_4, (27) and (28) can be numerically solved for the corresponding values of $C_{\mathcal{L}}$ and $C_{\mathcal{R}}$. Simple inspection of (27) and (28) indicates that interchanging values of $C_{\mathcal{L}}$ and $C_{\mathcal{R}}$ reverses the sign of τ_3 and has no effect on τ_4. Presented in Figure 2 (Panel B) is a graph of the region for possible combinations of $|\tau_3|$ and τ_4 in (27) and (28). Note that the graph in Figure 2 (Panel B) was drawn by setting $C_{\mathcal{L}} = 0$ with $C_{\mathcal{R}} \in [0, \infty)$ in (27) and (28). Also note that Figure 2 (Panel B) shows the minimum value of τ_4 for the double-SL PM distributions as $min(\tau_4) = 1/6$, where $C_{\mathcal{L}} = C_{\mathcal{R}} = C = 0$ and $\tau_3 = 0$, which are associated with the standard logistic pdf. The maximum value of τ_4 is $max(\tau_4) \approx .6733$, which is the limiting value of τ_4 in (28) when $C_{\mathcal{L}} = C_{\mathcal{R}} \to \infty$. The conventional moment based system for the double-SL PM distributions is given in Appendix C. This system was used to solve for the values of $C_{\mathcal{L}}$ and $C_{\mathcal{R}}$ for specified values of γ_3 and γ_4 associated with the distributions in Figure 4.These distributions are also used in simulation portion of the study in Section 4.

The unique solutions for $C_{\mathcal{L}}$ and $C_{\mathcal{R}}$ can be determined by evaluating the following expressions for given values of τ_3 and τ_4 as

$$C_{\mathcal{L}} = \frac{\pi^2\{(1 - 6\tau_4)\ln 4 + 5\tau_3\}}{3\{\pi^2(6\tau_4 - 1) - 30\}\ln 4} \tag{29}$$

$$C_{\mathcal{R}} = \frac{\pi^2\{(1 - 6\tau_4)\ln 4 - 5\tau_3\}}{3\{\pi^2(6\tau_4 - 1) - 30\}\ln 4} \tag{30}$$
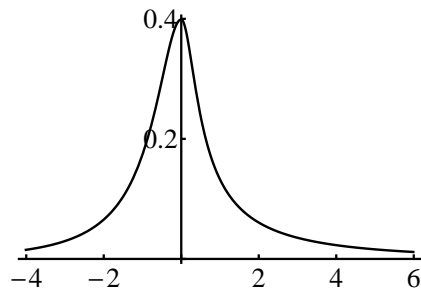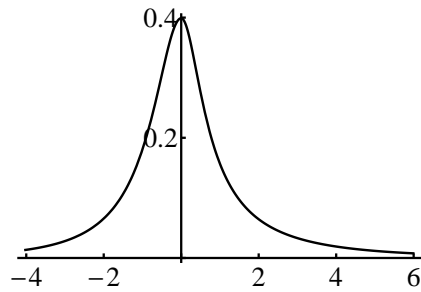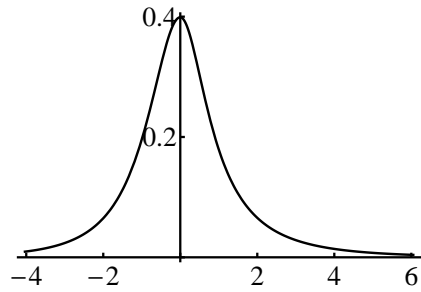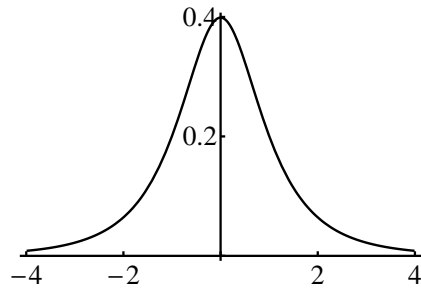
$$\gamma_3 = 4$$

$$\gamma_4 = 40$$

$$\tau_3 = 0.255884$$

$$\tau_4 = 0.400731$$

$$C_{\mathcal{L}} = 0.307610$$

$$\underline{C_{\mathcal{R}} = 0.985795}$$

Distribution 1

$$\gamma_3 = 2$$

$$\gamma_4 = 20$$

$$\tau_3 = 0.125230$$

$$\tau_4 = 0.340666$$

$$C_{\mathcal{L}} = 0.252815$$

$$\underline{C_{\mathcal{R}} = 0.498824}$$

Distribution 2

$$\gamma_3 = 1$$

$$\gamma_4 = 10$$

$$\tau_3 = 0.069541$$

$$\tau_4 = 0.277761$$

$$C_{\mathcal{L}} = 0.156646$$

$$\underline{C_{\mathcal{R}} = 0.264125}$$

Distribution 3

$$\gamma_3 = 0$$

$$\gamma_4 = 5$$

$$\tau_3 = 0$$

$$\tau_4 = 0.234240$$

$$C_{\mathcal{L}} = 0.131914$$

$$\underline{C_{\mathcal{R}} = 0.131914}$$

Distribution 4

Figure 3: Three asymmetric (Distributions 1-3) and one symmetric (Distribution 4) double-SN PM distributions with their conventional and L-moment parameters of skew (γ_3) and L-skew (τ_3), kurtosis (γ_4) and L-kurtosis (τ_4), and corresponding coefficients for equation (2).
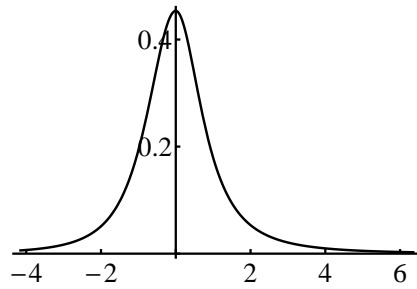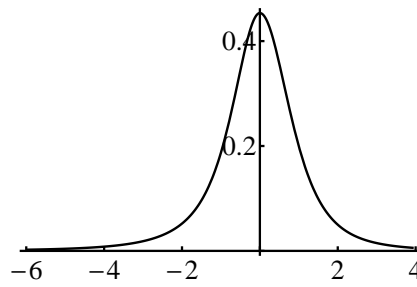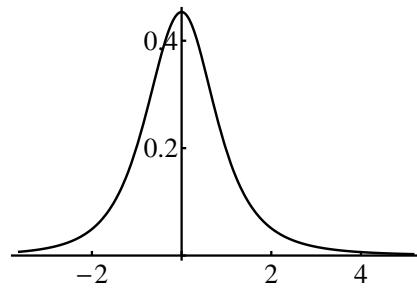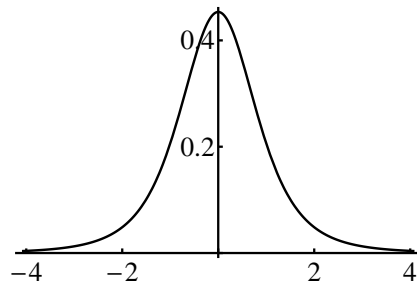
$$\gamma_3 = 3$$
$$\gamma_4 = 90$$
$$\tau_3 = 0.078748$$
$$\tau_4 = 0.317372$$
$$C_{\mathcal{L}} = 0.096814$$
$$\underline{C_{\mathcal{R}} = 0.185484}$$

Distribution 1

$$\gamma_3 = -2$$
$$\gamma_4 = 50$$
$$\tau_3 = -0.060691$$
$$\tau_4 = 0.281747$$
$$C_{\mathcal{L}} = 0.129036$$
$$\underline{C_{\mathcal{R}} = 0.066916}$$

Distribution 2

$$\gamma_3 = 1$$
$$\gamma_4 = 25$$
$$\tau_3 = 0.035521$$
$$\tau_4 = 0.253816$$
$$C_{\mathcal{L}} = 0.052287$$
$$\underline{C_{\mathcal{R}} = 0.086224}$$

Distribution 3

$$\gamma_3 = 0$$
$$\gamma_4 = 9$$
$$\tau_3 = 0$$
$$\tau_4 = 0.220193$$
$$C_{\mathcal{L}} = 0.039380$$
$$\underline{C_{\mathcal{R}} = 0.039380}$$

Distribution 4

Figure 4: Three asymmetric (Distributions 1-3) and one symmetric (Distribution 4) double-SL PM distributions with their conventional and L-moment parameters of skew (γ_3) and L-skew (τ_3), kurtosis (γ_4) and L-kurtosis (τ_4), and corresponding coefficients for equation (2).

3 Multivariate double-SN and SL PM distributions

3.1 Preliminaries : The L-correlation

The coefficient of L-correlation (see [31]) is defined by considering two random variables Y_j and Y_k with cdfs $F(Y_j)$ and $F(Y_k)$, respectively. The second L-moments of Y_j and Y_k can be expressed as

$$\lambda_2(Y_j) = 2\text{Cov}(Y_j, F(Y_j)) \tag{31}$$

$$\lambda_2(Y_k) = 2\text{Cov}(Y_k, F(Y_k)). \tag{32}$$

The second L-comoments of Y_j toward Y_k and Y_k toward Y_j are defined as

$$\lambda_2(Y_j, Y_k) = 2\text{Cov}(Y_j, F(Y_k)) \tag{33}$$

$$\lambda_2(Y_k, Y_j) = 2\text{Cov}(Y_k, F(Y_j)). \tag{34}$$

As such, the L-correlations of Y_j toward Y_k and Y_k toward Y_j are expressed as

$$\eta_{jk} = \frac{\lambda_2(Y_j, Y_k)}{\lambda_2(Y_j)} \tag{35}$$

$$\eta_{kj} = \frac{\lambda_2(Y_k, Y_j)}{\lambda_2(Y_k)}. \tag{36}$$

The L-correlation in (35) (or 36) is bounded such that $-1 \leq \eta_{jk} \leq 1$ where a value of $\eta_{jk} = 1(\eta_{jk} = -1)$ indicates a strictly increasing (decreasing) monotone relationship between the two variables. In general, we would also note that $\eta_{jk} \neq \eta_{kj}$.

3.2 The L-correlation for double-SN (or SL) PM distributions

In the context of L-moment based double-SN PM distributions, suppose it is desired to simulate T distributions based on (2) with a specified L-correlation matrix and where each distribution has its own specified values of τ_3 and τ_4. Define $p(Z_j)$ and $p(Z_k)$ as in (2) where Z_j and Z_k have intermediate (Pearson) correlation (IC) of r_{jk} and standard normal bivariate density of

$$f_{jk} = \{2\pi(1 - r_{jk}^2)^{1/2}\}^{-1}\exp\{-(z_j^2 + z_k^2 - 2r_{jk}z_jz_k)/\{2(1 - r_{jk}^2)^{1/2}\}\}. \tag{37}$$

Using (2), (35) with the denominator standardized to $\lambda_2 = 1/\sqrt{\pi}$ for the standard normal distribution, cdf of the standard normal distribution, and (37), the L-correlation of $p(Z_j)$ toward $p(Z_k)$ can be expressed as

$$
\begin{aligned}
\eta_{jk} &= 2\sqrt{\pi}\,\mathrm{Cov}\{x_j(p(Z_j)), F_{p(Z_k)}(p(Z_k))\} \\
&= 2\sqrt{\pi}\,\mathrm{Cov}\{x_j(p(Z_j)), \Phi(Z_k)\} \\
&= 2\sqrt{\pi}\int_{-\infty}^{+\infty}\int_{-\infty}^{+\infty} x_j(p(Z_j))\Phi(Z_k)f_{jk}dz_j dz_k
\end{aligned} \tag{38}
$$

where $x_j(p(Z_j))$ is the standardized piecewise function of $p(Z_j)$ in (2) such that it has a mean of zero and one-half the coefficient of mean difference equal to that of the standard normal distribution as

$$
x_j(p(Z_j)) = \delta(p(Z_j) - \lambda_1) \tag{39}
$$

where λ_1 is the mean from (10) and δ is a constant that scales λ_2 in (11) and in the denominator of (35) to $1/\sqrt{\pi}$ as

$$
\delta = 4/(4 + 5C_{\mathcal{L}} + 5C_{\mathcal{R}}) \tag{40}
$$

Analogously, the L-correlation of $p(Z_k)$ toward $p(Z_j)$ is

$$
\eta_{kj} = 2\sqrt{\pi}\int_{-\infty}^{+\infty}\int_{-\infty}^{+\infty} x_k(p(Z_k))\Phi(Z_j)f_{jk}dz_k dz_j. \tag{41}
$$

Given a specified value of η_{jk}, the intermediate correlation (r_{jk}) can be determined by solving equation (38) for r_{jk} using solved values of $C_{\mathcal{L}j}$ and $C_{\mathcal{R}j}$. Note that for the special case of where $C_{\mathcal{L}j} = C_{\mathcal{L}k}$ and $C_{\mathcal{R}j} = C_{\mathcal{R}k}$ in (38) and (41), then $\eta_{jk} = \eta_{kj}$. The details for simulating the double-SN (or SL) distributions with specified values of L-skew, L-kurtosis, and L-correlations are described in the next section.

4   The Procedure and Simulation Study

The procedure for simulating double-SN (or SL) PM distributions with specified L-moments and specified L-correlations is summarized in the following five (seven) steps:

1. Specify the L-moments for T transformations of the form in (2), i.e., $p(Z_1), \ldots, p(Z_T)$ for the double-SN $(p(W_1), \ldots, p(W_T)$ for the double-SL) and obtain the parameters of $C_{\mathcal{L}j}$ and $C_{\mathcal{R}j}$ by solving equations

(20) and (21) ((27) and (28)) using the specified values of L-skew (τ_3) and L-kurtosis (τ_4) for each distribution. Specify a $T \times T$ matrix of L-correlations (η_{jk}) for $p(Z_j)$ toward $p(Z_k)$ ($p(W_j)$ toward $p(W_k)$), where $j < k \in \{1, 2, \ldots, T\}$.

2. Compute the intermediate (Pearson) correlations (ICs), r_{jk}, by substituting the value of the specified L-correlation η_{jk} and the parameters of $C_{\mathcal{L}j}$ and $C_{\mathcal{R}j}$ from Step 1 into the left- and the right-hand sides of (38), respectively, and then numerically solve for r_{jk}. Repeat this step separately for all $T(T-1)/2$ pairwise combinations of ICs.

3. Assemble the solved values of ICs from Step 2 into a $T \times T$ matrix and decompose this matrix using a Cholesky factorization. Note that this step requires the IC matrix to be positive definite.

4. Use the results of the Cholesky factorization from Step 3 to generate T standard normal variables $(Z_1, \ldots, Z_T)$ correlated at the IC levels as follows:

$$
\begin{aligned}
Z_1 &= a_{11}V_1 \\
Z_2 &= a_{12}V_1 + a_{22}V_2 \\
&\;\;\vdots \\
Z_j &= a_{1j}V_1 + a_{2j}V_2 + \ldots + a_{ij}V_i + \ldots + a_{jj}V_j \\
&\;\;\vdots \\
Z_T &= a_{1T}V_1 + a_{2T}V_2 + \ldots + a_{iT}V_i + \ldots + a_{jT}V_j + \ldots + a_{TT}V_T
\end{aligned}
\tag{42}
$$

where $V_1, \ldots, V_T$ are independent standard normal random variables and where a_{ij} represents the element in the i-th row and the j-th column of the matrix associated with the Cholesky factorization performed in Step 3.

5. Substitute $Z_1, \ldots, Z_T$ from Step 4 into T equations of the form in (2), as noted in Step 1, to generate the non-normal double-SN PM distributions with the specified values of L-moments and L-correlations.

6. Substitute $Z_1, \ldots, Z_T$ from Step 4 into the following Taylor series-based expansion for the standard normal cdf, $\Phi(Z_j)$ [26]:

$$
\Phi(Z_j) = (1/2) + \phi(Z_j)\{Z_j + Z_j^3/3 + Z_j^5/(3 \cdot 5) + Z_j^7/(3 \cdot 5 \cdot 7) + \ldots\} \tag{43}
$$

where $\phi(Z_j)$ denotes the standard normal pdf and where the absolute error associated with (43) is less than 8×10^{-16}.

7. Substitute the zero-one uniform deviates, $\Phi(Z_j)$, generated from Step 6 into the T equations of the form $p(W_j)$ in (2), where $W_j = (\sqrt{3}/\pi)\ln\{\Phi(Z_j)/(1-\Phi(Z_j))\}$ is standard logistic deviate to generate the double-SL PM distributions with specified values of L-moments and L-correlations.

To demonstrate the steps above, and evaluate the proposed procedure, a comparison between the new L-moment and the conventional moment-based procedures is subsequently described. Specifically, the distributions in Figure 3 and Figure 4 are used as a basis for a comparison using the specified correlations in Table 3 where a mixture of moderate and strong correlations is considered in a single matrix. Presented in Matrix A (Matrix B) in Table 4 and Table 5 are the solved IC matrices for the conventional moment- and the L-moment-based procedures, respectively, for the distributions in Figure 3 (Figure 4). Figure 5 and Figure 6 (Figure 7 and Figure 8) provide Mathematica [38] algorithms and examples for computing ICs respectively for the L-moment- and the conventional moment-based procedures for distributions in Figure 3 (Figure 4). Table 6 and Table 7 provide the results of the Cholesky decompositions on the IC matrices, which are then used to create $Z_1, \ldots, Z_4$ with the solved ICs by making use of the formulae given in (42) of Step 4 with $T = 4$. The values of $Z_1, \ldots, Z_4$ are subsequently substituted into equations of the form in (2) to produce $p(Z_1), \ldots, p(Z_4)$ for both procedures for distributions in Figure 3. For generating distributions in Figure 4, however, two extra steps (e.g., Steps 6 and 7 above) are required. That is, (a) the values of $Z_1, \ldots, Z_4$ from Step 4 are substituted in (43) to obtain $\Phi(Z_1), \ldots, \Phi(Z_4)$, which are used (b) for generating four standard logistic variables $W_1, \ldots, W_4$ as described in Step 7, above. These standard logistic variables are subsequently substituted in $p(W_1), \ldots, p(W_4)$ of the form (2) to generate the four distributions in Figure 4.

In terms of the simulation, a Fortran algorithm was written for both procedures to generate 25,000 independent sample estimates for the specified parameters of: (a) conventional skew (γ_3), kurtosis (γ_4), and Pearson correlation (ρ_{jk}); and (b) L-skew (τ_3), L-kurtosis (τ_4), and L-correlation (η_{jk}) based on samples of sizes $n = 25$ and $n = 1000$. The estimates for $\gamma_{3,4}$ were based on Fisher's k-statistics, i.e., the formulae currently used by most commercial software packages such as SAS, SPSS, Minitab, etc., for computing indices of skew and kurtosis (where $\gamma_{3,4} = 0$ for the standard normal distribution). The formulae used for computing estimates for $\tau_{3,4}$ were Headrick's equations (2.4) and (2.6) [8]. The estimate for ρ_{jk} was based on the usual formula for the Pearson product-moment of correlation statistic and the estimate for η_{jk} was computed based on (38) using the empirical forms of the cdfs in (31) and (33). The estimates for ρ_{jk} and η_{jk} were both transformed using Fisher's z' transformation.

Bias-corrected accelerated bootstrapped average estimates, 95% confidence intervals (C.I.s), and standard errors (St. Error) were subsequently obtained for the estimates associated with the parameters $(\gamma_{3,4}, \tau_{3,4}, z'_{(\rho_{jk})}, z'_{(\eta_{jk})})$ using 10,000 resamples via the commercial software package Spotfire S+ [34]. The bootstrap results for the estimates of $z'_{(\rho_{jk})}$ and $z'_{(\eta_{jk})}$ were transformed back to their original metrics. Further, if a parameter (P) was outside its associated bootstrap C.I., then an index of relative bias (RB%) was computed for the estimate (E) as: RB% $= \{((E - P)/P) \times 100\}$. The results of the simulation are reported in Tables 12-13 and are discussed in the next section. Also provided in Tables 14-15, are the simulation results associated with Pearson and L-correlation estimates of distribution j toward distribution k for the four double-SL PM distributions in Figure 4.

	1	2	3	4
1	1			
2	0.65	1		
3	0.70	0.70	1	
4	0.85	0.70	0.80	1

Table 3: Specified correlation matrix for the conventional- and L-moment-based procedures for the distributions in Figure 3 and Figure 4.

	A			
	1	2	3	4
1	1			
2	0.734127	1		
3	0.781855	0.748604	1	
4	0.946869	0.753626	0.825323	1

	B			
	1	2	3	4
1	1			
2	0.737648	1		
3	0.762846	0.757042	1	
4	0.904769	0.746903	0.827009	1

Table 4: Intermediate correlation matrix A (B) for the conventional moment-based procedure for the distributions in Figure 3 (Figure 4).

	A			
	1	2	3	4
1	1			
2	0.602576	1		
3	0.653742	0.664034	1	
4	0.816350	0.664034	0.778880	1

	B			
	1	2	3	4
1	1			
2	0.612930	1		
3	0.664304	0.671261	1	
4	0.825357	0.671261	0.780879	1

Table 5: Intermediate correlation matrix A (B) for the *L*-moment-based procedure for the distributions in Figure 3 (Figure 4).

	A			
1	$a_{11} = 1$	$a_{12} = 0.734127$	$a_{13} = 0.781855$	$a_{14} = 0.946869$
2	0	$a_{22} = 0.679012$	$a_{23} = 0.257172$	$a_{24} = 0.086159$
3	0	0	$a_{33} = 0.567948$	$a_{34} = 0.110663$
4	0	0	0	$a_{44} = 0.289429$

	B			
1	$a_{11} = 1$	$a_{12} = 0.737648$	$a_{13} = 0.762846$	$a_{14} = 0.904769$
2	0	$a_{22} = 0.675186$	$a_{23} = 0.287817$	$a_{24} = 0.117748$
3	0	0	$a_{33} = 0.578988$	$a_{34} = 0.177757$
4	0	0	0	$a_{44} = 0.368688$

Table 6: Cholesky decomposition matrix A (B) for the conventional moment-based procedure for the distributions in Figure 3 (Figure 4).

5   Discussion

One of the advantages that *L*-moment ratios have over conventional moment-based estimators is that they can be far less biased when sampling is from distributions with more severe departures from normality ([21, 32]). Inspection of the simulation results in Table 8 and Table 9 (Table 10 and Table 11) clearly indicates that this is the case for the double-SN (double-SL) PM distributions. That is, the superiority that estimates of *L*-moment ratios (τ_3, τ_4) have over their corresponding conventional moment-based counterparts (γ_3, γ_4) is obvious. For example, with samples of size $n = 25$ the estimates of skew and kurtosis for Distribution 1 in Figure 3 (Figure 4) were, on average, only 34.5% (14.9%) and 14.9% (4.6%) of their associated population parameters whereas the estimates of *L*-skew and *L*-kurtosis were 85.66% (80.69%)

		A		
1	$a_{11} = 1$	$a_{12} = 0.602576$	$a_{13} = 0.653742$	$a_{14} = 0.816350$
2	0	$a_{22} = 0.798061$	$a_{23} = 0.338450$	$a_{24} = 0.215673$
3	0	0	$a_{33} = 0.676811$	$a_{34} = 0.254433$
4	0	0	0	$a_{44} = 0.471509$

		B		
1	$a_{11} = 1$	$a_{12} = 0.612930$	$a_{13} = 0.664304$	$a_{14} = 0.825357$
2	0	$a_{22} = 0.790137$	$a_{23} = 0.334231$	$a_{24} = 0.209299$
3	0	0	$a_{33} = 0.668572$	$a_{34} = 0.243260$
4	0	0	0	$a_{44} = 0.464548$

Table 7: Cholesky decomposition matrix A (B) for the L-moment-based procedure for the distributions in Figure 3 (Figure 4).

and 94.76% (92.50%) of their respective parameters. It is also evident from comparing Tables 8-11 that L-skew and L-kurtosis are more efficient estimators as their relative standard errors RSE $= \{(\text{St. Error/Estimate}) \times 100\}$ are considerably smaller than the conventional-moment based estimators of skew and kurtosis. For example, in terms of Distribution 1 in Figure 3, inspection of Table 8-B and Table 9-B indicates RSE measures of: $\text{RSE}(\hat{\gamma}_3) = 0.235\%$ and $\text{RSE}(\hat{\gamma}_4) = 0.508\%$ compared with $\text{RSE}(\hat{\tau}_3) = 0.079\%$ and $\text{RSE}(\hat{\tau}_4) = 0.025\%$. This demonstrates that L-skew and L-kurtosis have more precision because they have less variance around their estimates.

Presented in Tables 12-15 are the results associated with the conventional Pearson and L-correlations. Overall inspection of these tables indicates that the L-correlation is superior to the Pearson correlation in terms of relative bias. For example, for $n = 25$ the relative bias for the two heavy-tailed distributions (i.e., Distributions 1 and 2) in Figure 3 (Figure 4) was 8.32% (10.46%) for the Pearson correlation compared with only 0.91% (0.62%) for the L-correlation. It is also noted that the variability of the L-correlation appears to be more stable than that of the Pearson correlation both within and across different conditions.

In summary, the new L-moment-based procedure is an attractive alternative to the traditional conventional moment-based procedure. In particular, the L-moment based procedure has distinct advantages when distributions with large departures from normality are used. Finally, we note that Mathematica Version 8.0.1 [38] source code is available from the authors for implementing both the conventional and new L-moment-based procedures.

Dist	Parameter	Estimate	95% Bootstrap C.I.	St. Error	RB%
		A. $n = 25$			
1	$\gamma_3 = 4$	1.381	1.363, 1.401	0.0097	-65.5
	$\gamma_4 = 40$	5.979	5.916, 6.043	0.0325	-85.1
2	$\gamma_3 = 2$	0.717	0.698, 0.734	0.0092	-64.2
	$\gamma_4 = 20$	4.361	4.312, 4.410	0.0263	-78.2
3	$\gamma_3 = 1$	0.415	0.400, 0.430	0.0077	-58.5
	$\gamma_4 = 10$	2.970	2.930, 3.011	0.0213	-70.3
4	$\gamma_3 = 0$	0.009	-0.004, 0.021	0.0064	- - - -
	$\gamma_4 = 5$	2.003	1.972, 2.038	0.0168	-59.9

Dist	Parameter	Estimate	95% Bootstrap C.I.	St. Error	RB%
		B. $n = 1000$			
1	$\gamma_3 = 4$	3.619	3.601, 3.635	0.0085	-9.53
	$\gamma_4 = 40$	30.66	30.35, 30.96	0.1559	-23.4
2	$\gamma_3 = 2$	1.839	1.827, 1.852	0.0064	-8.05
	$\gamma_4 = 20$	16.82	16.65, 16.98	0.0853	-15.9
3	$\gamma_3 = 1$	0.941	0.933, 0.949	0.0042	-5.90
	$\gamma_4 = 10$	9.000	8.923, 9.081	0.0419	-10.0
4	$\gamma_3 = 0$	-0.001	-0.006, 0.004	0.0026	- - - -
	$\gamma_4 = 5$	4.738	4.706, 4.774	0.0175	-5.24

Table 8: Skew (γ_3) and kurtosis (γ_4) results for the distributions in Figure 3.

A. $n = 25$

Dist	Parameter	Estimate	95% Bootstrap C.I.	St. Error	RB%
1	$\tau_3 = 0.2559$	0.2192	0.2163, 0.2217	0.0014	-14.3
	$\tau_4 = 0.4007$	0.3797	0.3782, 0.3813	0.0008	-5.24
2	$\tau_3 = 0.1252$	0.1084	0.1061, 0.1111	0.0013	-13.4
	$\tau_4 = 0.3407$	0.3252	0.3238, 0.3266	0.0007	-4.55
3	$\tau_3 = 0.0695$	0.0617	0.0598, 0.0640	0.0011	-11.2
	$\tau_4 = 0.2778$	0.2675	0.2664, 0.2690	0.0007	-3.71
4	$\tau_3 = 0$	0.0011	-0.0006, 0.0030	0.0009	- - - -
	$\tau_4 = 0.2342$	0.2278	0.2266, 0.2290	0.0006	-2.73

B. $n = 1000$

Dist	Parameter	Estimate	95% Bootstrap C.I.	St. Error	RB%
1	$\tau_3 = 0.2559$	0.2546	0.2541, 0.2550	0.0002	-0.51
	$\tau_4 = 0.4007$	0.4001	0.3998, 0.4003	0.0001	-0.15
2	$\tau_3 = 0.1252$	0.1246	0.1242, 0.1250	0.0002	-0.48
	$\tau_4 = 0.3407$	0.3402	0.3400, 0.3404	0.0001	-0.15
3	$\tau_3 = 0.0695$	0.0692	0.0689, 0.0695	0.0002	-0.43
	$\tau_4 = 0.2778$	0.2775	0.2773, 0.2777	0.0001	-0.11
4	$\tau_3 = 0$	-0.0001	-0.0004, 0.0002	0.0002	- - - -
	$\tau_4 = 0.2342$	0.2341	0.2339, 0.2342	0.0001	-0.04

Table 9: *L*-skew (τ_3) and *L*-kurtosis (τ_4) results for the distributions in Figure 3.

A. $n = 25$

Dist	Parameter	Estimate	95% Bootstrap C.I.	St. Error	RB%
1	$\gamma_3 = 3$	0.447	0.427, 0.466	0.0097	-85.1
	$\gamma_4 = 90$	4.136	4.074, 4.191	0.0295	-95.4
2	$\gamma_3 = -2$	-0.333	-0.351, -0.317	0.0086	-83.4
	$\gamma_4 = 50$	3.310	3.261, 3.363	0.0260	-93.4
3	$\gamma_3 = 1$	0.218	0.201, 0.232	0.0079	-78.2
	$\gamma_4 = 25$	2.677	2.631, 2.721	0.0230	-89.3
4	$\gamma_3 = 0$	0.009	-0.004, 0.022	0.0065	- - - -
	$\gamma_4 = 9$	1.892	1.857, 1.928	0.0182	-79.0

B. $n = 1000$

Dist	Parameter	Estimate	95% Bootstrap C.I.	St. Error	RB%
1	$\gamma_3 = 3$	1.992	1.959, 2.024	0.0165	-33.6
	$\gamma_4 = 90$	35.87	35.26, 36.50	0.3195	-60.1
2	$\gamma_3 = -2$	-1.450	-1.475, -1.425	0.0127	-27.5
	$\gamma_4 = 50$	24.28	23.81, 24.73	0.2378	-51.4
3	$\gamma_3 = 1$	0.778	0.760, 0.795	0.0090	-22.2
	$\gamma_4 = 25$	15.19	14.90, 15.48	0.1481	-39.2
4	$\gamma_3 = 0$	-0.002	-0.012, 0.007	0.0050	- - - -
	$\gamma_4 = 9$	7.205	7.093, 7.343	0.0633	-19.9

Table 10: Skew (γ_3) and kurtosis (γ_4) results for the distributions in Figure 4.

	A. $n = 25$				
Dist	Parameter	Estimate	95% Bootstrap C.I.	St. Error	RB%
1	$\tau_3 = 0.0787$	0.0635	0.0610, 0.0661	0.0013	-19.3
	$\tau_4 = 0.3174$	0.2936	0.2921, 0.2951	0.0008	-7.50
2	$\tau_3 = -0.0607$	-0.0471	-0.0494, -0.0449	0.0011	-22.4
	$\tau_4 = 0.2817$	0.2636	0.2621, 0.2650	0.0007	-6.43
3	$\tau_3 = 0.0355$	0.0301	0.0281, 0.0322	0.0010	-15.2
	$\tau_4 = 0.2538$	0.2406	0.2393, 0.2419	0.0007	-5.20
4	$\tau_3 = 0$	0.0011	-0.0007, 0.0029	0.0009	- - - -
	$\tau_4 = 0.2202$	0.2122	0.2109, 0.2134	0.0006	-3.63

	B. $n = 1000$				
Dist	Parameter	Estimate	95% Bootstrap C.I.	St. Error	RB%
1	$\tau_3 = 0.0787$	0.0780	0.0775, 0.0785	0.0003	-0.89
	$\tau_4 = 0.3174$	0.3165	0.3162, 0.3168	0.0001	-0.28
2	$\tau_3 = -0.0607$	-0.0603	-0.0608, -0.0599	0.0002	-0.66
	$\tau_4 = 0.2817$	0.2811	0.2809, 0.2814	0.0001	-0.21
3	$\tau_3 = 0.0355$	0.0352	0.0348, 0.0356	0.0002	-0.85
	$\tau_4 = 0.2538$	0.2534	0.2532, 0.2536	0.0001	-0.16
4	$\tau_3 = 0$	-0.0001	-0.0004, 0.0003	0.0002	- - - -
	$\tau_4 = 0.2202$	0.2200	0.2198, 0.2201	0.0001	-0.09

Table 11: *L*-skew (τ_3) and *L*-kurtosis (τ_4) results for the distributions in Figure 4.

A. $n = 25$				
Parameter	Estimate	95% Bootstrap C.I.	St. Error	RB%
$\rho_{12} = 0.65$	0.7041	0.7021, 0.7060	0.00198	8.32
$\rho_{13} = 0.70$	0.7503	0.7487, 0.7519	0.00183	7.19
$\rho_{14} = 0.85$	0.9017	0.9012, 0.9023	0.00154	6.08
$\rho_{23} = 0.70$	0.7336	0.7321, 0.7352	0.00172	4.80
$\rho_{24} = 0.70$	0.7345	0.7331, 0.7359	0.00154	4.93
$\rho_{34} = 0.80$	0.8191	0.8181, 0.8200	0.00152	2.39

B. $n = 1000$				
Parameter	Estimate	95% Bootstrap C.I.	St. Error	RB%
$\rho_{12} = 0.65$	0.6531	0.6527, 0.6536	0.00042	0.48
$\rho_{13} = 0.70$	0.7034	0.7030, 0.7037	0.00038	0.49
$\rho_{14} = 0.85$	0.8540	0.8537, 0.8541	0.00037	0.47
$\rho_{23} = 0.70$	0.7014	0.7011, 0.7017	0.00033	0.20
$\rho_{24} = 0.70$	0.7018	0.7015, 0.7021	0.00029	0.26
$\rho_{34} = 0.80$	0.8009	0.8008, 0.8012	0.00027	0.11

Table 12: Correlation results for the conventional moment-based procedure for the double-SN PM distributions in Figure 3.

A. $n = 25$

Parameter	Estimate	95% Bootstrap C.I.	St. Error	RB%
$\eta_{12} = 0.65$	0.6559	0.6539, 0.6578	0.00171	0.91
$\eta_{13} = 0.70$	0.7051	0.7034, 0.7069	0.00173	0.73
$\eta_{14} = 0.85$	0.8530	0.8519, 0.8538	0.00171	0.35
$\eta_{23} = 0.70$	0.7046	0.7030, 0.7062	0.00159	0.66
$\eta_{24} = 0.70$	0.7044	0.7028, 0.7060	0.00157	0.63
$\eta_{34} = 0.80$	0.8048	0.8038, 0.8059	0.00150	0.60

B. $n = 1000$

Parameter	Estimate	95% Bootstrap C.I.	St. Error	RB%
$\eta_{12} = 0.65$	0.6499	0.6496, 0.6502	0.00027	- - - -
$\eta_{13} = 0.70$	0.7001	0.6998, 0.7004	0.00027	- - - -
$\eta_{14} = 0.85$	0.8500	0.8498, 0.8501	0.00026	- - - -
$\eta_{23} = 0.70$	0.6998	0.6995, 0.7000	0.00024	- - - -
$\eta_{24} = 0.70$	0.6999	0.6997, 0.7001	0.00024	- - - -
$\eta_{34} = 0.80$	0.8001	0.7999, 0.8002	0.00022	- - - -

Table 13: Correlation results for the L-moment-based procedure for the double-SN PM distributions in Figure 3.

A. $n = 25$

Parameter	Estimate	95% Bootstrap C.I.	St. Error	RB%
$\rho_{12} = 0.65$	0.7180	0.7165, 0.7196	0.00165	10.46
$\rho_{13} = 0.70$	0.7512	0.7499, 0.7527	0.00168	7.31
$\rho_{14} = 0.85$	0.8923	0.8916, 0.8929	0.00161	4.98
$\rho_{23} = 0.70$	0.7460	0.7446, 0.7473	0.00157	6.57
$\rho_{24} = 0.70$	0.7387	0.7372, 0.7399	0.00153	5.53
$\rho_{34} = 0.80$	0.8240	0.8229, 0.8248	0.00152	3.00

B. $n = 1000$

Parameter	Estimate	95% Bootstrap C.I.	St. Error	RB%
$\rho_{12} = 0.65$	0.6599	0.6594, 0.6604	0.00046	1.52
$\rho_{13} = 0.70$	0.7073	0.7069, 0.7078	0.00045	1.04
$\rho_{14} = 0.85$	0.8578	0.8574, 0.8580	0.00055	0.92
$\rho_{23} = 0.70$	0.7055	0.7051, 0.7059	0.00039	0.79
$\rho_{24} = 0.70$	0.7046	0.7042, 0.7049	0.00035	0.66
$\rho_{34} = 0.80$	0.8026	0.8023, 0.8028	0.00034	0.33

Table 14: Correlation results for the conventional moment-based procedure for the double-SL PM distributions in Figure 4.

A. $n = 25$				
Parameter	Estimate	95% Bootstrap C.I.	St. Error	RB%
$\eta_{12} = 0.65$	0.6540	0.6523, 0.6559	0.00159	0.62
$\eta_{13} = 0.70$	0.7035	0.7018, 0.7049	0.00158	0.50
$\eta_{14} = 0.85$	0.8524	0.8516, 0.8534	0.00161	0.28
$\eta_{23} = 0.70$	0.7042	0.7026, 0.7056	0.00153	0.60
$\eta_{24} = 0.70$	0.7044	0.7029, 0.7058	0.00152	0.63
$\eta_{34} = 0.80$	0.8051	0.8040, 0.8061	0.00151	0.64

B. $n = 1000$				
Parameter	Estimate	95% Bootstrap C.I.	St. Error	RB%
$\eta_{12} = 0.65$	0.6498	0.6496, 0.6501	0.00025	- - - -
$\eta_{13} = 0.70$	0.7001	0.6998, 0.7003	0.00025	- - - -
$\eta_{14} = 0.85$	0.8500	0.8499, 0.8501	0.00024	- - - -
$\eta_{23} = 0.70$	0.6997	0.6995, 0.7000	0.00023	- - - -
$\eta_{24} = 0.70$	0.6999	0.6997, 0.7001	0.00024	- - - -
$\eta_{34} = 0.80$	0.8001	0.7998, 0.8002	0.00023	- - - -

Table 15: Correlation results for the L-moment-based procedure for the double-SL PM distributions in Figure 4.

(* The subscripts j and k represent distributions 1 and 2 in Figure 3 *)

$\Phi_k = \text{CDF}[\text{NormalDistribution}[0, 1], Z_k]$;

Needs["MultivariateStatistics`"];

$f_{jk} = \text{PDF}\left[\text{MultinormalDistribution}\left[\{0, 0\}, \left\{\{1, r_{jk}\}, \{r_{jk}, 1\}\right\}\right], \{Z_j, Z_k\}\right]$;

(* Coefficients for distribution 1 in Figure 3 *)

$C_{\mathcal{L}j} = 0.3076104045682757$;

$C_{\mathcal{R}j} = 0.9857945062541974$;

$Y_{\mathcal{L}j} = Z_j + C_{\mathcal{L}j} \times Z_j^3$;

$Y_{\mathcal{R}j} = Z_j + C_{\mathcal{R}j} \times Z_j^3$;

$p_j = \text{Piecewise}\left[\left\{\{Y_{\mathcal{L}j},\ Z_j \leq 0\}, \{Y_{\mathcal{R}j},\ Z_j > 0\}\right\}\right]$;

(* Mean and the standardizing constant for distribution 1 in Figure 3 *)

$\lambda_j = \sqrt{(2/\pi)}\left(C_{\mathcal{R}j} - C_{\mathcal{L}j}\right)$;

$\delta_j = 4/\left(4 + 5C_{\mathcal{L}j} + 5C_{\mathcal{R}j}\right)$;

(* Intermediate correlation *)

$r_{jk} = 0.602576253341645$;

(* Computed value of the specified L-correlation *)

$\eta_{jk} = 2\sqrt{\pi} \times \text{NIntegrate}\left[\left(\delta_j \times \left(p_j - \lambda_j\right)\right) \times \Phi_k \times f_{jk}, \{z_j, -\infty, \infty\}, \{z_k, -\infty, \infty\}\right]$

0.65

Figure 5: Mathematica [38] source code for computing intermediate correlations for the specified L-correlations. The example is for the specified L-correlation (η_{12}) of distribution $j = 1$ toward distribution $k = 2$ in Figure 3. See also Table 3 and Table 5 (matrix A).

(* The subscripts j and k represent distributions 1 and 2 in Figure 3 *)

Needs["MultivariateStatistics`"];

$f_{jk} = \text{PDF}\left[\text{MultinormalDistribution}\left[\{0,0\}, \{\{1, r_{jk}\}, \{r_{jk}, 1\}\}\right], \{Z_j, Z_k\}\right];$

(* Solved values of coefficients for distributions 1 and 2 in Figure 3 *)

$C_{\mathcal{L}j} = 0.3076104045682757;$

$C_{\mathcal{R}j} = 0.9857945062541974;$

$C_{\mathcal{L}k} = 0.2528148933949333;$

$C_{\mathcal{R}k} = 0.4988239303169917;$

$Y_{\mathcal{L}j} = Z_j + C_{\mathcal{L}j} \times Z_j^3;$

$Y_{\mathcal{R}j} = Z_j + C_{\mathcal{R}j} \times Z_j^3;$

$Y_{\mathcal{L}k} = Z_k + C_{\mathcal{L}k} \times Z_k^3;$

$Y_{\mathcal{R}k} = Z_k + C_{\mathcal{R}k} \times Z_k^3;$

$p_j = \text{Piecewise}\left[\{\{Y_{\mathcal{L}j}, \ Z_j \leq 0\}, \{Y_{\mathcal{R}j}, \ Z_j > 0\}\}\right];$

$p_k = \text{Piecewise}\left[\{\{Y_{\mathcal{L}k}, \ Z_k \leq 0\}, \{Y_{\mathcal{R}k}, \ Z_k > 0\}\}\right];$

(* Standardizing distributions 1 and 2 using μ_j, μ_k from (56) and σ_j, σ_k from (57) of the Appendix B *)

$Sp_j = (p_j - \mu_j)/\sigma_j;$

$Sp_k = (p_k - \mu_k)/\sigma_k;$

(* Intermediate Correlation *)

$r_{jk} = 0.7341272544619965;$

(* Computed value of the specified Pearson correlation *)

$\eta_{jk} = \text{NIntegrate}\left[Sp_j \times Sp_k \times f_{jk}, \{z_j, -\infty, \infty\}, \{z_k, -\infty, \infty\}\right]$

0.65

Figure 6: Mathematica [38] source code for computing intermediate correlations for specified Pearson correlations. The example is for the specified Pearson correlation (ρ_{12}) between distributions $j = 1$ and $k = 2$ in Figure 3. See also Table 3 and Table 4 (matrix A).

(* The subscripts j and k represent distributions 1 and 2 in Figure 4 *)

$\Phi_j = \text{CDF}\big[\text{NormalDistribution}[0,1], Z_j\big]$;

$\Phi_k = \text{CDF}\big[\text{NormalDistribution}[0,1], Z_k\big]$;

$W_j = \left(\sqrt{3}/\pi\right)\text{Log}\big[\Phi_j/(1-\Phi_j)\big]$;

$W_k = \left(\sqrt{3}/\pi\right)\text{Log}\big[\Phi_k/(1-\Phi_k)\big]$;

$F_k = 1/\big(1 + \text{Exp}\big[(-\pi/\sqrt{3})W_k\big]\big)$;

Needs["MultivariateStatistics`"];

$f_{jk} = \text{PDF}\Big[\text{MultinormalDistribution}\Big[\{0,0\}, \big\{\{1, r_{jk}\}, \{r_{jk}, 1\}\big\}\Big], \{Z_j, Z_k\}\Big]$;

(* Coefficients for distribution 1 in Figure 4 *)

$C_{\mathcal{L}j} = 0.09681373923131754$;

$C_{\mathcal{R}j} = 0.18548440821382653$;

$Y_{\mathcal{L}j} = W_j + C_{\mathcal{L}j} \times W_j^3$;

$Y_{\mathcal{R}j} = W_j + C_{\mathcal{R}j} \times W_j^3$;

$p_j = \text{Piecewise}\Big[\big\{\{Y_{\mathcal{L}j}, W_j \leq 0\}, \{Y_{\mathcal{R}j}, W_j > 0\}\big\}\Big]$;

(* Mean and the standardizing constant for distribution 1 in Figure 4 *)

$\lambda_j = \big(27\sqrt{3}(C_{\mathcal{R}j} - C_{\mathcal{L}j})\text{Zeta}[3]\big)/(2\pi^3)$;

$\delta_j = \left(2\sqrt{\pi/3}\right)/(2 + 3C_{\mathcal{L}j} + 3C_{\mathcal{R}j})$;

(* Intermediate correlation *)

$r_{jk} = 0.612930311888817$;

(* Computed value of the specified L-correlation *)

$\eta_{jk} = 2\sqrt{\pi} \times \text{NIntegrate}\Big[\big(\delta_j \times (p_j - \lambda_j)\big) \times F_k \times f_{jk}, \{z_j, -\infty, \infty\}, \{z_k, -\infty, \infty\}\Big]$

0.65

Figure 7: Mathematica [38] source code for computing intermediate correlations for the specified L-correlations. The example is for the specified L-correlation (η_{12}) of distribution $j = 1$ toward distribution $k = 2$ in Figure 4. See also Table 3 and Table 5 (matrix B).

(* The subsripts j and k represent distributions 1 and 2 in Figure 4 *)

$\Phi_j = \text{CDF}\big[\text{NormalDistribution}[0,1], Z_j\big];$

$\Phi_k = \text{CDF}[\text{NormalDistribution}[0,1], Z_k];$

$W_j = (\sqrt{3}/\pi)\,\text{Log}\big[\Phi_j/(1-\Phi_j)\big];$

$W_k = (\sqrt{3}/\pi)\,\text{Log}[\Phi_k/(1-\Phi_k)];$

Needs["MultivariateStatistics`"];

$f_{jk} = \text{PDF}\Big[\text{MultinormalDistribution}\Big[\{0,0\}, \big\{\{1, r_{jk}\}, \{r_{jk}, 1\}\big\}\Big], \{Z_j, Z_k\}\Big];$

(* Solved values of coefficients for distributions 1 and 2 in Figure 4 *)

$C_{\mathcal{L}j} = 0.09681373923131754;$

$C_{\mathcal{R}j} = 0.18548440821382653;$

$C_{\mathcal{L}k} = 0.12903624455950970;$

$C_{\mathcal{R}k} = 0.06691567859544602;$

$Y_{\mathcal{L}j} = W_j + C_{\mathcal{L}j} \times W_j^3;$

$Y_{\mathcal{R}j} = W_j + C_{\mathcal{R}j} \times W_j^3;$

$Y_{\mathcal{L}k} = W_k + C_{\mathcal{L}k} \times W_k^3;$

$Y_{\mathcal{R}k} = W_k + C_{\mathcal{R}k} \times W_k^3;$

$p_j = \text{Piecewise}\Big[\big\{\{Y_{\mathcal{L}j},\ W_j \le 0\}, \{Y_{\mathcal{R}j},\ W_j > 0\}\big\}\Big];$

$p_k = \text{Piecewise}\big[\big\{\{Y_{\mathcal{L}k},\ W_k \le 0\}, \{Y_{\mathcal{R}k},\ W_k > 0\}\big\}\big];$

(* Standardizing distributions 1 and 2 using μ_j, μ_k from (61) and σ_j, σ_k from (62) of the Appendix C *)

$Sp_j = (p_j - \mu_j)/\sigma_j;$

$Sp_k = (p_k - \mu_k)/\sigma_k;$

(* Intermediate Correlation *)

$r_{jk} = 0.7376479346883659;$

(* Computed value of the specified Pearson correlation *)

$\eta_{jk} = \text{NIntegrate}\big[Sp_j \times Sp_k \times f_{jk}, \{z_j, -10, 10\}, \{z_k, -10, 10\}\big]$

0.65

Figure 8: Mathematica [38] source code for computing intermediate correlations for specified Pearson correlations. The example is for the specified Pearson correlation (ρ_{12}) between distributions $j = 1$ and $k = 2$ in Figure 4. See also Table 3 and Table 4 (matrix B).

References

[1] J. Affleck-Graves and B. MacDonald, Nonnormalities and tests of asset pricing theories, *Journal of Finance,* **44** (1989), 889 - 908.

[2] T.M. Beasley and B.D. Zumbo, Comparison of aligned Friedman rank and parametric methods for testing interactions in split-plot designs, *Computational Statistics and Data Analysis,* **42** (2003), 569 - 593.

[3] I. Berkovits, G.R. Hancock and J. Nevitt, Bootstrap resampling approaches for repeated measures designs: relative robustness to sphericity and normality violations, *Educational and Psychological Measurement,* **60** (2000), 877 - 892.

[4] A.I. Fleishman, A method for simulating non-normal distributions, *Psychometrika,* **43** (1978), 521 - 532.

[5] M.R. Harwell and R.C. Serlin, An empirical study of a proposed test of nonparametric analysis of covariance, *Psychological Bulletin,* **104** (1988), 268 - 281.

[6] T.C. Headrick, Fast fifth-order polynomial transforms for generating univariate and multivariate non-normal distributions, *Computational Statistics and Data Analysis,* **40** (2002), 685 - 711.

[7] T.C. Headrick, *Statistical Simulation: Power Method Polynomials and Other Transformations,* Chapman & Hall /CRC, Boca Raton, FL, 2010.

[8] T.C. Headrick, A characterization of power method transformations through *L*-moments, *Journal of Probability and Statistics,* **vol. 2011**, Article ID 497463, 22 pages, 2011.

[9] T.C. Headrick and M.D. Pant, On the order statistics of standard normal-based power method distributions, *ISRN Applied Mathematics,* **vol. 2012**, Article ID 945627, 13 pages, 2012.

[10] T.C. Headrick and O. Rotou, An investigation of the rank transformation in multiple regression, *Computational Statistics and Data Analysis,* **38** (2001), 203 - 225.

[11] T.C. Headrick and S.S. Sawilowsky, Simulating correlated multivariate non-normal distributions, *Psychometrika,* **64** (1999), 25 - 35.

[12] T.C. Headrick and S.S. Sawilowsky, Properties of the rank transformation in factorial analysis of covariance, *Communications in Statistics: Simulation and Computation,* **29** (2000), 1059 - 1087.

[13] T.C. Headrick, R.K. Kowalchuk and Y. Sheng, Parametric probability densities and distribution functions for Tukey *g*-and-*h* transformations and their use for fitting data, *Applied Mathematical Sciences,* **2** (2008), 449 - 462.

[14] J.M. Henson, S.P. Reise and K.H. Kim, Detecting mixtures from structural model differences using latent variable mixture modeling: A comparison of relative model fit statistics, *Structural Equation Modeling,* **14** (2007), 202 - 226.

[15] G.D. Hess and S. Iwata, Measuring and comparing business-cycle features, *Journal of Business and Economic Statistics,* **15** (1997), 432 - 444.

[16] F.A. Hodis, T.C. Headrick and Y. Sheng, Power method distributions through conventional moments and *L*-moments, *Applied Mathematical Sciences,* **6** (2012), 2159 - 2193.

[17] L. Hothorn and W. Lehmacher, A simple testing procedure "control versus *k* treatments" for one-sided ordered alternatives, with application in toxicology, *Biometrical Journal,* **33** (2007), 179 - 189.

[18] J.R.M. Hosking, *L*-moments: Analysis and estimation of distributions using linear combinations of order statistics, *Journal of the Royal Statistical Society, Series B,* **52** (1990), 105 - 124.

[19] J.R.M. Hosking, Moments or *L*-moments? An example comparing two measures of distributional shape, *American Statistician,* **46** (1992), 186 - 189.

[20] J.R.M. Hosking, Some theory and practical uses of trimmed *L*-moments, *Journal of Statistical Planning and Inference,* **137** (2007), 3024 - 3039.

[21] J.R.M. Hosking and J.R. Wallis, *Regional Frequency Analysis: An Approach Based on L-Moments*, Cambridge University Press, Cambridge, UK, 1997.

[22] M.C. Jones, On some expressions for variance, covariance, skewness, and *L*-moments, *Journal of Statistical Planning and Inference,* **126** (2004), 97 - 106.

[23] H.J. Keselman, R.R. Wilcox, J. Algina, A.R. Othman and K. Fradette, A comparitive study of robust tests for spread: asymmetric trimming strategies, *The British Journal of Mathematical and Statistical Psychology,* **61** (2008), 235 - 253.

[24] L.M. Lix and R.T. Fouladi, Robust step-down tests for multivariate independent group designs, *The British Journal of Mathematical and Statistical Psychology,* **60** (2007), 245 - 265.

[25] O. Mahul, Hedging price risk in the presence of crop yield and revenue insurance, *European Review of Agricultural Economics,* **30** (2003), 217 - 239.

[26] G. Marsaglia, Evaluating the normal distribution, *Journal of Statistical Software,* **11** (2004), 1 - 11.

[27] S. Morgenthaler and J.W. Tukey, Fitting quantiles: Doubling, HR, HQ, and HHH distributions, *Journal of Computational and Graphical Statistics,* **9** (2000), 180 - 195.

[28] A. Nataf, Determination des distributions de probabilites dont les marges sont donnees, *BComptes Rendus de L'Academie des Sciences,* **225** (1962), 42 - 43.

[29] M.D. Pant, *Simulating univariate and multivariate Burr Type III and Type XII distributions through the method of L-moments,* Ph.D. Dissertation, Southern Illinois University Carbondale, http://opensiuc.lib.siu.edu/dissertations/401/, 2011.

[30] D.A. Powell, L.M. Anderson, R.Y. Cheng and W.G. Alvord, Robustness of the Chen-Dougherty-Bittner procedure against non-normality and heterogeneity distribution in the coefficient of variation, *Journal of Biomedical Optics,* **7** (2002), 650 - 660.

[31] R. Serfling and P. Xiao, A contribution to multivariate *L*-moments: *L*-comoment matrices, *Journal of Multivariate Analysis,* **98** (2007), 1765 - 1781.

[32] H.S. Steyn, On the problem of more than one kurtosis parameter in multivariate analysis, *Journal of Multivariate Analysis,* **44** (1993), 1 - 22.

[33] C.A. Stone, Empirical power and type I error rates for an IRT fit statistic that considers the precision of ability estimates, *Educational and Psychological Measurement,* **63** (2003), 566 - 583.

[34] TIBCO, *Spotfire S+ 8.1 for Windows,* TIBCO Software, Palo Alto, CA, 2008.

[35] C.D. Vale and V.A. Maurelli, Simulating multivariate nonnormal distributions, *Psychometrika,* **48** (1983), 465 - 471.

[36] M. Vorechovsky and D. Novak, Correlation control in small-sample Monte Carlo type simulations I: A simulated annealing approach, *Probabilistic Engineering Mechanics,* **24** (2009), 452 - 462.

[37] S. Wolfram, *The Mathematica Book,* 5th ed., Wolfram Media, Champaign, IL, 2003.

[38] Wolfram Research Inc., *Mathematica,* Version 8.0.1, Wolfram Research Inc., Champaign, IL, 2010.

Appendices

A Evaluation of integrals in equation (12)

The integrals I_1 and I_3 in equation (12) can be evaluated using integration by parts, where $u = \{\Phi(z)\}^2$ and $dv = z\phi(z)dz$ yield $du = 2\Phi(z)\phi(z)dz$ and $v = -\phi(z)$, as

$$
\begin{aligned}
I_1 &= \int_{-\infty}^{0} \{\Phi(z)\}^2 d(-\phi(z)) \\
&= -\{\Phi(z)\}^2\phi(z)|_{-\infty}^{0} + 2\int_{-\infty}^{0} \Phi(z)\{\phi(z)\}^2 dz \\
&= -\frac{1}{4\sqrt{2\pi}} + \frac{2}{\sqrt{2\pi}}\int_{-\infty}^{0} \Phi(z)\frac{1}{\sqrt{2\pi}}\exp\left\{-\frac{(\sqrt{2}z)^2}{2}\right\}dz \\
&= -\frac{1}{4\sqrt{2\pi}} + \frac{2}{\sqrt{2\pi}}\int_{-\infty}^{0} \Phi(z)\phi(\sqrt{2}z)dz \\
&= -\frac{1}{4\sqrt{2\pi}} + \frac{2}{\sqrt{2\pi}}I_5
\end{aligned}
\tag{44}
$$

$$
\begin{aligned}
I_3 &= \int_{0}^{\infty} \{\Phi(z)\}^2 d(-\phi(z)) \\
&= -\{\Phi(z)\}^2\phi(z)|_{0}^{\infty} + 2\int_{0}^{\infty} \Phi(z)\{\phi(z)\}^2 dz \\
&= \frac{1}{4\sqrt{2\pi}} + \frac{2}{\sqrt{2\pi}}\int_{0}^{\infty} \Phi(z)\frac{1}{\sqrt{2\pi}}\exp\left\{-\frac{(\sqrt{2}z)^2}{2}\right\}dz \\
&= \frac{1}{4\sqrt{2\pi}} + \frac{2}{\sqrt{2\pi}}\int_{0}^{\infty} \Phi(z)\phi(\sqrt{2}z)dz \\
&= \frac{1}{4\sqrt{2\pi}} + \frac{2}{\sqrt{2\pi}}I_6
\end{aligned}
\tag{45}
$$

If we let $\sqrt{2}z = X \sim N(0, 1/2)$ and $z = Y \sim N(0, 1)$, where X and Y are independent such that $(X/\sqrt{2}, Y)$ jointly have standard bivariate normal distribution, then the integrals I_5 and I_6 in (44) and (45) can be evaluated as

$$
\begin{aligned}
I_5 &= \int_{-\infty}^{0} \Phi(z)\phi(\sqrt{2}z)dz \\
&= \Pr\{X < 0, Y < X\} \\
&= \Pr\{X/\sqrt{2} < 0, Y < \sqrt{2}(X/\sqrt{2})\} \\
&= \frac{\tan^{-1}(\sqrt{2})}{2\sqrt{2}\pi}
\end{aligned}
\tag{46}
$$

$$
\begin{aligned}
I_6 &= \int_0^\infty \Phi(z)\phi(\sqrt{2}z)dz \\
&= \Pr\{0 < X < \infty, 0 < Y < X\} \\
&= \Pr\{0 < (X/\sqrt{2}) < \infty, 0 < Y < \sqrt{2}(X/\sqrt{2})\} \\
&= \frac{\pi - \tan^{-1}(\sqrt{2})}{2\sqrt{2}\pi}
\end{aligned}
\tag{47}
$$

The integrals I_2 and I_4 in equation (12) can be evaluated using integration by parts, where $u = \{\Phi(z)\}^2$ and $dv = z^3\phi(z)dz$ yield $du = 2\Phi(z)\phi(z)dz$ and $v = -(2+z^2)\phi(z)$, as

$$
\begin{aligned}
I_2 &= \int_{-\infty}^0 z^3\{\Phi(z)\}^2\phi(z)dz \\
&= -\int_{-\infty}^0 \{\Phi(z)\}^2 d((2+z^2)\phi(z)) \\
&= -\{\Phi(z)\}^2(2+z^2)\phi(z)|_{-\infty}^0 + 2\int_{-\infty}^0 \Phi(z)(2+z^2)\{\phi(z)\}^2 dz \\
&= -\frac{1}{2\sqrt{2\pi}} + \frac{2}{\sqrt{2\pi}}\int_{-\infty}^0 \Phi(z)(\frac{5}{2}-\frac{1}{2}+z^2)\frac{1}{\sqrt{2\pi}}\exp\{-\frac{1}{2}(\sqrt{2}z)^2\}dz \\
&= -\frac{1}{2\sqrt{2\pi}} + \frac{5}{\sqrt{2\pi}}\int_{-\infty}^0 \Phi(z)\phi(\sqrt{2}z)dz + \frac{2}{\sqrt{2\pi}}\int_{-\infty}^0 \Phi(z)(z^2-\frac{1}{2})\phi(\sqrt{2}z)dz \\
&= -\frac{1}{2\sqrt{2\pi}} + \frac{5}{\sqrt{2\pi}}I_5 + \frac{2}{\sqrt{2\pi}}I_7
\end{aligned}
\tag{48}
$$

$$
\begin{aligned}
I_4 &= \int_0^\infty z^3\{\Phi(z)\}^2\phi(z)dz \\
&= -\int_0^\infty \{\Phi(z)\}^2 d((2+z^2)\phi(z)) \\
&= -\{\Phi(z)\}^2(2+z^2)\phi(z)|_0^\infty + 2\int_0^\infty \Phi(z)(2+z^2)\{\phi(z)\}^2 dz \\
&= \frac{1}{2\sqrt{2\pi}} + \frac{2}{\sqrt{2\pi}}\int_0^\infty \Phi(z)(\frac{5}{2}-\frac{1}{2}+z^2)\frac{1}{\sqrt{2\pi}}\exp\{-\frac{1}{2}(\sqrt{2}z)^2\}dz \\
&= \frac{1}{2\sqrt{2\pi}} + \frac{5}{\sqrt{2\pi}}\int_0^\infty \Phi(z)\phi(\sqrt{2}z)dz + \frac{2}{\sqrt{2\pi}}\int_0^\infty \Phi(z)(z^2-\frac{1}{2})\phi(\sqrt{2}z)dz \\
&= \frac{1}{2\sqrt{2\pi}} + \frac{5}{\sqrt{2\pi}}I_6 + \frac{2}{\sqrt{2\pi}}I_8
\end{aligned}
\tag{49}
$$

The integrals I_7 and I_8 in equations (48) and (49) are such that $I_7 = -I_8$ and as such I_7 can be evaluated using integration by parts, where $u = \Phi(z)$ and $dv = (z^2 - 1/2)\phi(\sqrt{2}z)dz$ yield $du = \phi(z)dz$ and $v = (-z/2)\phi(\sqrt{2}z)$, as

$$
I_7 = \int_{-\infty}^0 \Phi(z)(z^2 - \frac{1}{2})\phi(\sqrt{2}z)dz
$$

$$
\begin{aligned}
&= -\int_{-\infty}^{0} \Phi(z)d(\frac{z}{2}\phi(\sqrt{2}z)) \\
&= -\frac{z}{2}\Phi(z)\phi(\sqrt{2}z)|_{-\infty}^{0} + \frac{1}{2}\int_{-\infty}^{0} z\phi(\sqrt{2}z)\phi(z)dz \\
&= \frac{1}{2}\int_{-\infty}^{0} \frac{z}{\sqrt{2\pi}}\exp\{-\frac{(\sqrt{2}z)^2}{2}\}\frac{1}{\sqrt{2\pi}}\exp\{-\frac{z^2}{2}\}dz \\
&= \frac{1}{4\pi}\int_{-\infty}^{0} z \times \exp\{-\frac{3z^2}{2}\}dz \\
&= \frac{1}{12\pi}\int_{-\infty}^{0} \exp\{-\frac{3z^2}{2}\}d(\frac{3z^2}{2}) \\
&= -\frac{1}{12\pi} \qquad\qquad (50) \\
&= -I_8.
\end{aligned}
$$

Thus, substituting (46) into (44), (46) and (50) into (48), (47) into (45), and (47) and (50) into (49), and simplifying gives the integrals I_1, I_2, I_3, and I_4 in their simplified forms as:

$$
I_1 = -\frac{1}{4\sqrt{2\pi}} + \frac{\tan^{-1}(\sqrt{2})}{2\pi\sqrt{\pi}} \tag{51}
$$

$$
I_2 = \frac{15\tan^{-1}(\sqrt{2}) - \sqrt{2} - 3\sqrt{2}\pi}{12\pi^{3/2}} \tag{52}
$$

$$
I_3 = \frac{1}{4\sqrt{2\pi}} + \frac{\pi - \tan^{-1}(\sqrt{2})}{2\pi\sqrt{\pi}} \tag{53}
$$

$$
I_4 = \frac{15(\pi - \tan^{-1}(\sqrt{2})) + \sqrt{2}(1 + 3\pi)}{12\pi^{3/2}}. \tag{54}
$$

B Conventional moment-based system of equations for the double-SN PM distributions.

The conventional moments $(\mu_{r=1,\ldots,4})$ associated with equation (2) can be obtained from

$$
\mu_r = \int_{-\infty}^{0} (z + C_{\mathcal{L}}z^3)^r \phi(z)dz + \int_{0}^{\infty} (z + C_{\mathcal{R}}z^3)^r \phi(z)dz. \tag{55}
$$

The mean (μ), variance (σ^2), skew (γ_3), and kurtosis (γ_4) are based on the formulae given in Headrick et al. [13, equations (16)-(18)]

$$
\mu = -\frac{1 + 2C_{\mathcal{L}}}{\sqrt{2\pi}} + \frac{1 + 2C_{\mathcal{R}}}{\sqrt{2\pi}} \tag{56}
$$

$$\sigma^2 = \frac{A}{2} = \frac{-4(C_{\mathcal{L}} - C_{\mathcal{R}})^2 + (2 + 3C_{\mathcal{L}}(2 + 5C_{\mathcal{L}}) + 3C_{\mathcal{R}}(2 + 5C_{\mathcal{R}}))\pi}{2\pi} \quad (57)$$

$$
\begin{aligned}
\gamma_3 = {}& -2(C_{\mathcal{L}} - C_{\mathcal{R}})[8(C_{\mathcal{L}} - C_{\mathcal{R}})^2 + 3\{6 + 113C_{\mathcal{L}}^2 \\
& + 2C_{\mathcal{L}}(21 + 64C_{\mathcal{R}}) + C_{\mathcal{R}}(42 + 113C_{\mathcal{R}})\}\pi]/(A\pi)^{3/2} \quad (58)
\end{aligned}
$$

$$
\begin{aligned}
\gamma_4 = {}& [3\{-48(C_{\mathcal{L}} - C_{\mathcal{R}})^4 - 8(C_{\mathcal{L}} - C_{\mathcal{R}})^2\{11 + 211C_{\mathcal{L}}^2 \\
& + C_{\mathcal{R}}(78 + 211C_{\mathcal{R}}) + C_{\mathcal{L}}(78 + 256C_{\mathcal{R}})\}\pi + \{2304C_{\mathcal{L}}^3 + 6705C_{\mathcal{L}}^4 \\
& - 18C_{\mathcal{L}}^2(5C_{\mathcal{R}}(2 + 5C_{\mathcal{R}}) - 18) - 4C_{\mathcal{L}}(9C_{\mathcal{R}}(2 + 5C_{\mathcal{R}}) - 4) \\
& + C_{\mathcal{R}}\{16 + 9C_{\mathcal{R}}(36 + 5C_{\mathcal{R}}(52 + 149C_{\mathcal{R}}))\}\}\pi^2\}]/(A\pi)^2 \quad (59)
\end{aligned}
$$

C Conventional moment-based system of equations for the double-SL PM distributions.

The conventional moments $(\mu_{r=1,\dots,4})$ associated with equation (2) can be obtained from

$$\mu_r = \int_{-\infty}^{0} (w + C_{\mathcal{L}}w^3)^r \phi(w)dw + \int_{0}^{\infty} (w + C_{\mathcal{R}}w^3)^r \phi(w)dw. \quad (60)$$

The mean (μ), variance (σ^2), skew (γ_3), and kurtosis (γ_4) are based on the formulae given in Headrick et al. [13, equations (16)-(18)]

$$\mu = \frac{27\sqrt{3}(C_{\mathcal{R}} - C_{\mathcal{L}})Z[3]}{2\pi^3} \quad (61)$$

$$\sigma^2 = 1 + \frac{3C_{\mathcal{L}}(98 + 465C_{\mathcal{L}}) + 3C_{\mathcal{R}}(98 + 465C_{\mathcal{R}})}{70} \quad (62)$$
$$- \frac{2187(C_{\mathcal{L}} - C_{\mathcal{R}})^2 Z[3]^2}{4\pi^6}$$

$$
\begin{aligned}
\gamma_3 = {}& [162\sqrt{105}(C_{\mathcal{L}} - C_{\mathcal{R}})\{(70 + 3C_{\mathcal{L}}(98 + 465C_{\mathcal{L}}) \\
& + 3C_{\mathcal{R}}(98 + 465C_{\mathcal{R}}))\pi^6 Z[3] - 5250\pi^4 Z[5] \\
& - 694575(C_{\mathcal{L}} + C_{\mathcal{R}})\pi^2 Z[7] + 8505\{-3(C_{\mathcal{L}} - C_{\mathcal{R}})^2 Z[3]^3 \\
& - 5950(C_{\mathcal{L}}^2 + C_{\mathcal{L}}C_{\mathcal{R}} + C_{\mathcal{R}}^2)Z[9]\}\}]/(140\sqrt{140}\pi^9 \sigma^3) \quad (63)
\end{aligned}
$$

$$
\begin{aligned}
\gamma_4 = {}& \{\{-3(70 + 3C_{\mathcal{L}}(98 + 465C_{\mathcal{L}}) + 3C_{\mathcal{R}}(98 + 465C_{\mathcal{R}}))^2/4900\} \\
& + \{3\{14014 + 3C_{\mathcal{L}}(88660 + 9C_{\mathcal{L}}(254254 \\
& + C_{\mathcal{L}}(4650100 + 46677741C_{\mathcal{L}}))) + 3C_{\mathcal{R}}(88660
\end{aligned}
$$

$$+9C_{\mathcal{R}}(254254 + C_{\mathcal{R}}(4650100 + 46677741C_{\mathcal{R}})))\}/10010\}$$
$$+(70 + 3C_{\mathcal{L}}(98 + 465C_{\mathcal{L}}) + 3C_{\mathcal{R}}(98 + 465C_{\mathcal{R}}))$$
$$\times\{6561(C_{\mathcal{R}} - C_{\mathcal{L}})^2Z[3]^2/(70\pi^6)\}$$
$$-\{14348907(C_{\mathcal{R}} - C_{\mathcal{L}})^4Z[3]^4/(8\pi^{12})\}$$
$$-\{98415(C_{\mathcal{R}} - C_{\mathcal{L}})^2Z[3]/(2\pi^{12})\}$$
$$\times\{10\pi^4Z[5] + 1323(C_{\mathcal{L}} + C_{\mathcal{R}})\pi^2Z[7] + 96390(C_{\mathcal{L}}^2$$
$$+C_{\mathcal{L}}C_{\mathcal{R}} + C_{\mathcal{R}}^2)Z[9]\}\}/\sigma^4 \tag{64}$$

where the notation Z[.] in equations (61)-(64) is the zeta function.

D Conventional moment-based procedure for computing intermediate (Pearson) correlation for the double-SN PM distributions.

Let $p(Z_j)$ and $p(Z_k)$ be two random variables of the form in equation (2) that are correlated at the specified Pearson correlation level of ρ_{jk}. Let Z_j and Z_k be correlated at the intermediate correlation level of r_{jk}, with the joint pdf given as in equation (37). The specified Pearson correlation ρ_{jk} between $p(Z_j)$ and $p(Z_k)$ is given by

$$\begin{aligned}
\rho_{jk} &= \mathrm{Cov}\left(\frac{p(Z_j) - \mu_j}{\sigma_j}, \frac{p(Z_k) - \mu_k}{\sigma_k}\right) \\
&= \int_{-\infty}^{+\infty}\int_{-\infty}^{+\infty}\left(\frac{p(z_j) - \mu_j}{\sigma_j}\right)\left(\frac{p(z_k) - \mu_k}{\sigma_k}\right)f_{jk}dz_jdz_k.
\end{aligned} \tag{65}$$

where μ_j and μ_k are the means, and σj and σ_k are the standard deviations associated with $p(Z_j)$ and $p(Z_k)$, which can be obtained from equations (56) and (57) of the Appendix B. Also, note that $p(Z_j)$ and $p(Z_k)$ can be expressed as piecewise functions in Mathematica [37] source code as in Figure 6.

Substituting the value of specified correlation ρ_{jk} on the left-hand side and solved values of $C_{\mathcal{L}}$ and $C_{\mathcal{R}}$ and equation (37) on the right-hand side of equation (65) and then numerically integrate equation (65) for $T(T - 1)/2$ intermediate correlations r_{jk} so that T specified double-SN PM distributions also have a specified correlation structure.

E   Conventional moment-based procedure for computing intermediate (Pearson) correlation for the double-SL PM distributions.

Let $p(W_j)$ and $p(W_k)$ be two random variables of the form in equation (2) that are correlated at the specified Pearson correlation level of ρ_{jk}. Let $W_j = (\sqrt{3}/\pi)\ln\{\Phi(Z_j)/(1-\Phi(Z_j))\}$ and $W_k = (\sqrt{3}/\pi)\ln\{\Phi(Z_k)/(1-\Phi(Z_k))\}$ be two standard logistic random variables, where $\Phi(Z_j)$ and $\Phi(Z_k)$ are the cdfs associated with standard normal variables Z_j and Z_k. Let Z_j and Z_k be correlated at the intermediate correlation level of r_{jk}, with the joint pdf given as in equation (37). The specified Pearson correlation ρ_{jk} between $p(W_j)$ and $p(W_k)$ is given by

$$
\begin{aligned}
\rho_{jk} &= \text{Cov}\left(\frac{p(W_j) - \mu_j}{\sigma_j}, \frac{p(W_k) - \mu_k}{\sigma_k}\right) \\
&= \int_{-\infty}^{+\infty} \int_{-\infty}^{+\infty} \left(\frac{p(w_j) - \mu_j}{\sigma_j}\right)\left(\frac{p(w_k) - \mu_k}{\sigma_k}\right) f_{jk} dz_j dz_k.
\end{aligned}
\tag{66}
$$

where μ_j and μ_k are the means, and σj and σ_k are the standard deviations associated with $p(W_j)$ and $p(W_k)$, which can be obtained from equations (61) and (62) of the Appendix C. Also, note that $p(W_j)$ and $p(W_k)$ can be expressed as piecewise functions in Mathematica [37] source code as in Figure 8.

Substituting the value of specified correlation ρ_{jk} on the left-hand side and solved values of $C_{\mathcal{L}}$ and $C_{\mathcal{R}}$ and equation (37) on the right-hand side of equation (66) and then numerically integrate equation (66) for $T(T-1)/2$ intermediate correlations r_{jk} so that T specified double-SL PM distributions also have a specified correlation structure.

Received: August 03, 2012